Journal of Molecular Graphics and Modelling 28 (2010) 495–505

Contents lists available at ScienceDirect

Journal of Molecular Graphics and Modelling

journal homepage: www.elsevier.com/locate/JMGM

Structural comparison of μ-opioid receptor selective peptides confirmed four parameters of bioactivity

Attila Borics *, Géza Tóth

Institute of Biochemistry, Biological Research Center of the Hungarian Academy of Sciences, 62 Temesvári körút, Szeged H-6720, Hungary

ARTICLE INFO

Article history:
Received 10 August 2009
Received in revised form 24 November 2009
Accepted 27 November 2009
Available online 3 December 2009

Keywords:
μ-Opioid
Peptide
Endomorphin
Structure
Conformation
Molecular dynamics

ABSTRACT

Structural determinants of binding to the μ-opioid receptor, an important target in analgesia, attract great scientific attention. Many natural and synthetic peptides and peptidomimetics were shown previously to bind to this receptor selectively but there is no consensus about the structure responsible for biological activity. No high resolution structure of this receptor is available and the binding site of ligands is not exactly known. However, μ-opioid ligands with similar affinity and selectivity should possess at least one common structural feature. Comparative structural analysis of such ligands, considering adequate representation of binding conditions, may reveal key features of bioactivity. In this study ten μ-opioid receptor ligands, DAMGO, Tyr-W-MIF-1, morphiceptin, endomorphin-1 and 2 and their analogues, possessing different affinity and selectivity, were examined using molecular dynamics. Conformational preference of these molecules was determined in H_2O and DMSO along with structural properties previously proposed to be important for binding. Four of such structural requirements were confirmed to be important, providing a possible structural model of receptor binding. Simultaneous fulfillment of these requirements results most likely in high affinity binding to the μ-opioid receptor.

1. Introduction

The μ-opioid receptor (MOR) is an important target in the search for novel analgesics. Thus structural determinants of binding to this receptor attract considerable scientific attention [1–6]. Endomorphin-1 (EM-1) and endomorphin-2 (EM-2) were proposed in the past decade as endogenous ligands of the MOR, characterized by their exceptionally high affinity and selectivity [7]. In addition, several modified opioid peptides were shown previously to bind to the MOR selectively, such as DAMGO [8], morphiceptin [9] and disulfide bridged cyclic analogues of somatostatin [10,11]. The members of the Tyr-MIF-1 family [12,13] were the first hypothalamic peptides which were shown to act also in the brain besides the pituitary. Investigation of this family established the field of selective endogenous opioid peptides and eventually led to the discovery of EMs. This opened a new era in the development of novel analgesics and tremendous efforts were taken to substitute morphine with novel EM-based painkillers devoid of dramatic side effects. Because of their short *in vivo* half-life [14] exogenous application of synthetic neuropeptides to suppress chronic pain is greatly limited. To increase stability against proteases while maintaining opioid activity, hundreds of synthetic analogues of EM-1 and EM-2 were prepared by inserting non-natural amino acid residues [15–25], introducing conformational constraints [26–29], modifying peptide bonds [30] and by designing stereoisomers [31] or peptidomimetics [32–34]. Many promising μ-selective analogues were found but in most cases structural modifications led to decreased selectivity toward the MOR. Nevertheless, these findings are of great importance and provided further information about possible structural requirements of binding to opioid receptors (vide infra).

Endogenous opioid peptides are flexible as short peptides are in general. According to the message-address concept [35] opioid sequences can be subdivided into two functional parts. The message part, usually the N-terminal part of the sequence, is necessary for recognition, while the address part provides selectivity. However, these sub-units vary greatly among different opioids. By general consensus the phenolic OH group of an N-terminal Tyr residue with a free cationic α-amino group (similar to the tyramine moiety of morphine) and an aromatic amino acid separated by one or two residues are the key requirements for the binding of opioid peptides [36–38] (Fig. 1). Additionally, a polar but not acidic C-terminal function was found to be essential for MOR binding of EMs [17]. A structural model of μ-opioid activity was first proposed based on ^{1}H-NMR studies of morphiceptin and its stereoisomeric analogues. The distances between the three

* Corresponding author. Tel.: +36 62 599 600x582; fax: +36 62 433 506.
E-mail address: aborics@brc.hu (A. Borics).

1093-3263/$ – see front matter © 2009 Elsevier Inc. All rights reserved.
doi:10.1016/j.jmgm.2009.11.006

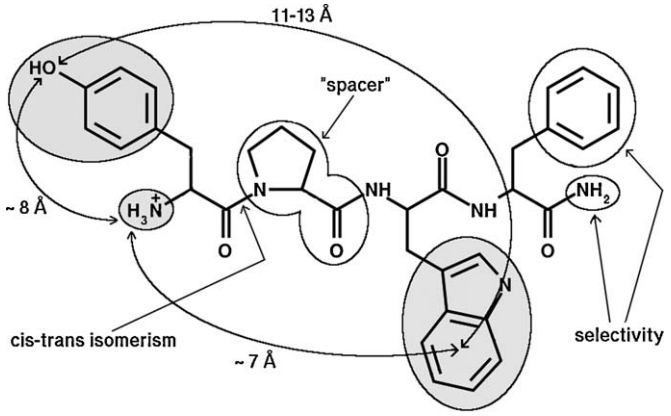

Fig. 1. General structural characteristics and pharmacophore definition of μ-opioid receptor ligands, shown on the example of endomorphin-1 (EM-2, **2**). Important chemical moieties are circled and pharmacophore groups are additionally highlighted. Pharmacophore distances proposed by Yamazaki et al. [37] are also shown.

pharmacophore groups, Tyr^1 N to Tyr^1 OH, Tyr^1 N to the center of Phe^3 aromatic ring and Tyr^1 OH to the center of Phe^3 aromatic ring were found to be ~8, ~7 and ~11–13 Å, respectively [37]. Another topographical model of MOR selective ligands was proposed based on the structural analysis of cyclic somatostatin analogues. In that model the optimal spatial arrangement of pharmacophores is furnished by bent backbone structure and *gauche+* conformation, *gauche−* conformation and increased flexibility of the first, second and third aromatic side chains, respectively [39].

The solution structure of EMs and their analogues, in relation with their bioactivity, was investigated extensively and the results were summarized in excellent reviews [29,40], but the backbone and side-chain conformation responsible for the μ-opioid activity of EM-1 and EM-2 is still debated. There is no agreement about whether peptides bind to the MOR in an extended- [41,43] or in a more compact, bent [25,26,32] backbone structure, since both conformational families are readily accessible for EMs and other short opioid peptides in solution [43,44,45]. It was shown, that the peptide bond preceding Pro^2 in the EMs is prone to *cis*/*trans* isomerization [41,42] and there is exclusive experimental evidence in support of both the *cis* [16] and the *trans* [25,26] conformer. Synthesis and biological evaluation of stereoisomeric analogues of EM-2 showed that different stereoisomers adopt different backbone structures, which results in remarkable variation of bioactivity [31]. However, a stereodiversified library of 1,5-enediol-based MOR ligands did not demonstrate such high diversity of MOR affinity [33,34]. As well as previously proposed topographical models [37,39] the solution conformation of the aromatic side chains of EMs and other MOR ligands were determined in numerous studies and several suggestions were given for their conformation in the receptor-bound structural state [17,24,38,44,46]. Generally, the flexibility of side chains, or in other words the free rotation around the χ^1 side-chain torsional angle was found to increase from the N- to the C-terminus in the EMs and the Pro^2 residue was suggested to function as a stereochemical spacer, responsible for the proper orientation of the pharmacophore groups [38]. Another important property of aromatic side chains is that they stabilize local structures [38] through various aromatic–aromatic and aromatic–proline interactions [47] which results in slightly lower backbone flexibility compared to other peptides of this size. Nevertheless, backbone and side-chain conformations of MOR ligands should not be examined and discussed separately as they contribute concurrently to the orientation of pharmacophore groups. Furthermore, a similar spatial arrangement of pharmacophores may be achieved through more than one combination of backbone- and side-chain conformations [38].

Receptor-based investigation of possible binding modes of ligands is difficult, because no high resolution experimental structure of the MOR is available. Structural models of the MOR as a member of the G-protein coupled receptor superfamily were proposed based on the X-ray crystallographic structure of bovine rhodopsin, electron cryomicroscopic studies, site-directed mutagenesis results and the analysis of variability and hydrophobicity patterns [48–54]. However, sequence similarity between the MOR and rhodopsin is approximately 20% which may lead to unrealistic assumptions about the position and chemical environment of the putative binding pocket in MOR models. Chimeric and point mutated receptors were constructed to locate regions which are responsible for ligand binding [55–59]. While several amino acid residues and loop regions were identified to be essential for ligand binding, it is still difficult to determine the exact location of a binding site. This supports the emerging concept that the receptor possesses considerable plasticity in ligand engagement [52,53] and suggests that studies of opioid activity should rather focus on the structure of ligands. Identification of possible structure–activity relationships is supported by a tremendous amount of biological data available for various EM-1 and EM-2 analogues. MOR ligands with similar affinity should possess at least one common structural feature in which they differ from other ligands of different affinity. Comparative structural analysis of such ligands may reveal key features of bioactivity. Such a ligand-based study was performed partly by our group previously and a slightly bent backbone structure was proposed for receptor-bound ligands [43]. The receptor-bound structure proposed in that study was in agreement with a rhodopsin-based receptor–ligand complex model [54].

Structural studies of biologically relevant molecules involve the adequate representation of binding conditions. The fundamental question is what solvent environment has to be employed and how does that possibly relate to the microscopic environment in which the action of the studied molecule is exerted. Since an unambiguously confirmed MOR–ligand complex model has not yet been published, different environmental conditions of receptor binding have to be taken into account. In other words, it is not known if ligands bind on the surface of the MOR or immerse into the transmembrane region. Therefore the use of solvents mimicking intersynaptic transport fluid, membrane- and protein environment has to be considered. Water is used generally as the paradigmatic biological environment but intersynaptic fluids have much higher viscosity and lower relative permittivity [60]. These two physical parameters can have a dramatic influence on the conformational equilibrium of short peptides. In high viscosity fluids conformational transitions are much slower, while lower relative permittivity modulates intra- and intermolecular electrostatic interactions significantly. Several solvents and solvent mixtures were proposed previously to mimic various biological environments [60,61]. Dimethyl-sulfoxide (DMSO) was shown to be a fairly good physical approximation to transport fluid environments as it has lower relative permittivity and higher viscosity, in the range of that of intersynaptic fluids. Moreover, being a good hydrogen bond acceptor, DMSO induces rather inter- than intramolecular interactions, which may reveal intrinsic conformational preferences and may mimic the physical circumstances of receptor–ligand interactions [61]. Many may dispute this latter statement and refer to DMSO as a denaturing agent despite the fact that it is routinely used as solvent for NMR spectroscopic studies and there is experimental evidence of folded structures in DMSO [60,61].

In this study 150 ns molecular dynamics (MD) simulations were performed in a comparative manner for ten previously proposed MOR ligands [7–9,13,25,26], listed in Table 1. This structurally

Table 1
μ-Opioid receptor ligands addressed in this study.

	Ligand	Sequence	Receptor affinity (K_i^{μ}/nM)	μ/δ selectivity (K_i^{δ}/K_i^{μ})
1	EM-1	H-Tyr-Pro-Trp-Phe-NH_2	0–10	>1000
2	EM-2	H-Tyr-Pro-Phe-Phe-NH_2	0–10	>1000
3	DAMGO	H-Tyr-D-Ala-Gly-*N*-Me-Phe-Gly-ol	0–10	1000–100
4	(1*S*,2*R*)-ACHC^2-EM-2	H-Tyr-(1*S*2*R*)-ACHC-Phe-Phe-NH_2	0–10	1000–100
5	Tyr-W-MIF-1	H-Tyr-Pro-Trp-Gly-NH_2	10–100	1000–100
6	(*R*)-spiro-Aba^2-Gly^3-EM-2	H-Tyr-(*R*)-spiro-Aba-Gly-Phe-NH_2	10–100	>1000
7	Morphiceptin	H-Tyr-Pro-Phe-Pro-NH_2	10–100	1000–100
8	(1*R*,2*R*)-ACPC^2-EM-1	H-Tyr-(1*R*2*R*)-ACPC-Trp-Phe-NH_2	10–100	100–10
9	(1*R*,2*S*)-ACHC^2-EM-2	H-Tyr-(1*R*2*S*)-ACHC-Phe-Phe-NH_2	100–1000	>1000
10	(*S*)-Aba^2-Gly^3-EM-2	H-Tyr-(*R*)-spiro-Aba-Gly-Phe-NH_2	100–1000	<10

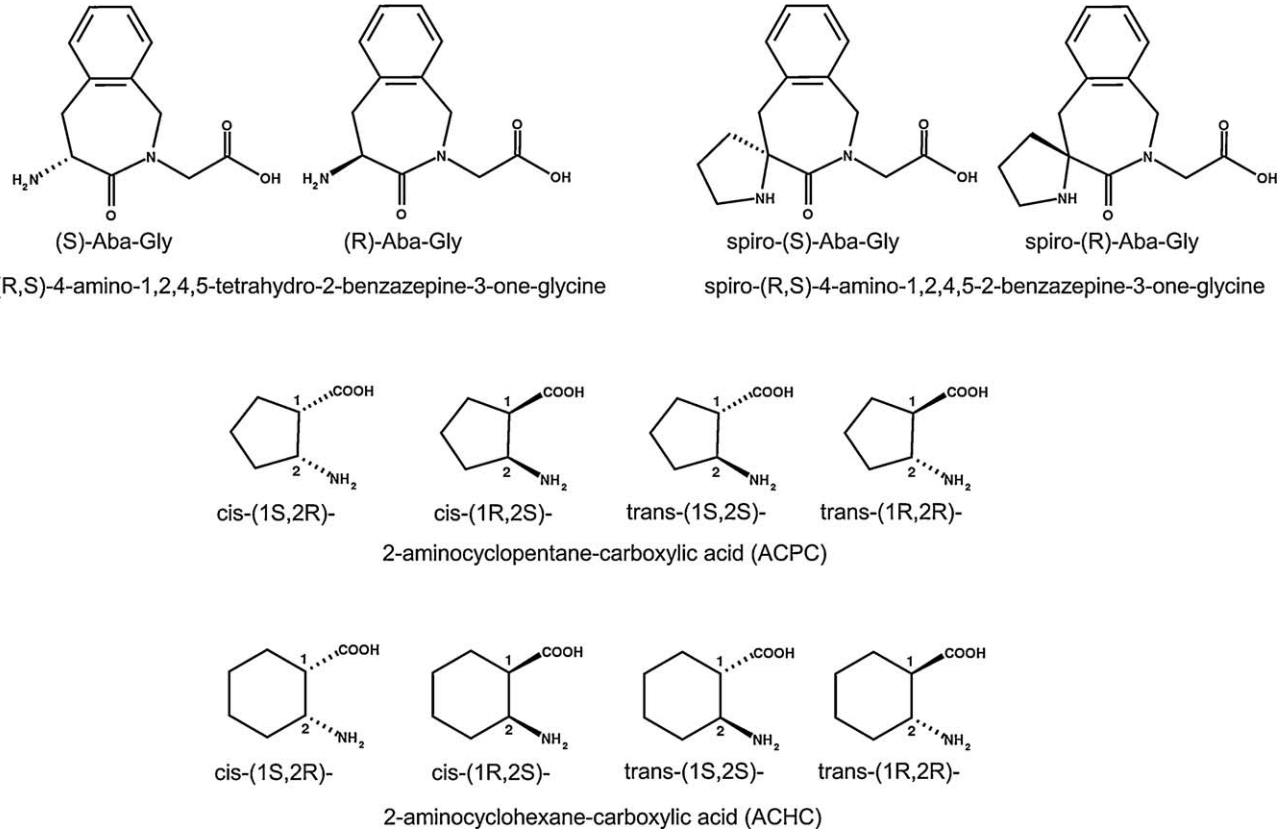

Fig. 2. Pseudo-dipeptides and alicyclic β-amino acids, incorporated in compounds **4**, **6**, **8**, **9** and **10**.

diverse (Fig. 2) pool of ligands can be divided into three groups of different MOR affinity. Conformational preference of the elements of these groups was determined in aqueous and DMSO media. Since the spatial orientation of pharmacophore groups determine the ability of ligands to bind to the receptor and this orientation is primarily governed by backbone and side-chain conformations, these structural parameters were the focus of analysis.

2. Methods

Starting structures for MD simulations were obtained by performing distance geometry calculations using the TINKER 4.2 program package [62]. 1000 structures were generated for each peptide where the peptide bond between Tyr^1 and the second residue was kept in either *cis*- or *trans* configuration. For peptides which demonstrated the predominance of *trans* configuration in previous experimental studies [25–26] only those conformers were generated. Resultant structures were clustered to identify and eliminate duplicate structures from further analysis. Clustering was performed using the g_cluster utility of the GROMACS 3.3 program package [63], and the gromos [64] method with 0.5 Å RMSD similarity cut-off comparing positions of backbone atoms, amide hydrogens, amide carbonyl oxygens and β-carbon atoms. Only the middle structures of the resultant clusters were subjected to further analysis. These geometries were energy minimized using the AMBER 9 program package [65], the generalized Amber force field (gAFF) [66] and the GB/SA implicit solvent model [67]. 1000 steps of steepest descent, followed by 1500 steps of conjugate gradient minimization was done where the convergence criteria for the energy gradient was 10^{-4} kcal mol^{-1} Å and the long-range non-bonded interactions were calculated within a 10 Å cut-off distance. The resultant pool of structures was clustered again as described above to identify and eliminate structures which correspond to the same local energy minimum. The middle structures of these final clusters, which were regarded as possible geometries of the studied peptides, were analyzed one by one,

using the VMD and the Molekel molecular visualization and analysis programs. For each peptide only three markedly different low-energy structures were found. Thus three simulations were started either from extended, γ-turn or β-turn or bent structures.

MD simulations were performed using the AMBER 9 program package and the AMBER ff99 force field parameter set [68]. Parameters for unnatural amino acid residues were supplemented from the gAFF and partial charges were determined at the HF/6-31G(d) level using the RESP method. Peptides were immersed in a truncated octahedral box of pre-equilibrated TIP3P water [69] or DMSO molecules [70] where the box sides were at least 10 Å from the closest atom of the solute. Solvent molecules were removed from the box when the distance between any atom of the solute molecule and any atom of the solvent molecule was less than the sum of the Van der Waals radii of both atoms. Charged N-termini of peptides were neutralized by Cl^- ions at the positions of the first solvent molecule with the most favorable electrostatic potential. All systems were subjected to 500 steps of steepest descent followed by 500 steps of conjugate gradient energy minimization having all atoms of the solute molecule fixed with a 500 kcal mol^{-1} $Å^2$ force constant. Then the position restraint was removed and 1000 steps of steepest descent, followed by 1500 steps of conjugate gradient energy minimization were performed on the whole system. 100 ps NVT molecular dynamics was then performed with slow heating from 0 to 300 K and by positionally restraining the peptide in the center of the box with a force constant of 10 kcal mol^{-1} $Å^2$ on each atom to allow the solvent density to equilibrate around the solute molecule. This was followed by 50.25 ns NPT molecular dynamics simulations of each system at constant temperature (300 K) and pressure (1 bar), with the following parameters: the time step was set to 2 fs, the SHAKE algorithm was used to constrain all bonds to their correct lengths, temperature was regulated with the weak coupling algorithm with a relaxation constant of 1.0 ps, constant pressure was maintained using isotropic scaling with a relaxation constant of 2.0 ps and 4.46×10^{-5} and 5.25×10^{-5} bar^{-1} isothermal compressibility for water and DMSO, respectively. Non-bonded interactions were calculated using the PME method with all cut-off values set at 10 Å. The coordinates of the system were stored after every 2 ps and trajectories were combined with the first 250 ps excluded, which were regarded as the equilibration period. This resulted in 150 ns trajectories of 75,000 sampled conformations for each peptide.

All analysis was done using programs of the GROMACS 3.3 suite and Perl scripts written in-house. Structures along the trajectory were probed for the existence of intramolecular hydrogen bonds by the g_hbond utility of GROMACS 3.3. The cut-off distance between a donor and an acceptor atom was set to 3.5 Å and 60° was used as the cut-off for the donor–hydrogen–acceptor angle. The secondary structure of peptides with a native backbone was assigned using the STRIDE algorithm [71]. The backbone structure was also examined through the measurement of the N(1)-C_α(2)-C_α(3)-C(4) virtual dihedral angle and the distance between the terminal C_α-atoms [72]. A bent structure was assigned, when this dihedral angle was between −80° and 80° and the distance was less than 7 Å. Distances between the putative pharmacophoric elements [37] and side-chain rotamer populations were also determined utilizing the g_dist and g_chi programs, respectively. Coordinates of a rhodopsin-based MOR–ligand complex model were acquired from the webpage of the Mosberg group [54]. Receptor–ligand complexes, which were built based on the results of this study were refined by 500 steps of steepest descent energy minimization, using the AMBER 9 package and the AMBER ff99 force field. Atomic coordinates of the MOR were held rigid during the minimization by a positional restraint described above. Figures depicting molecular structure were prepared using the Pymol software [73].

3. Results

3.1. Backbone conformation

STRIDE secondary structural analysis of the conformational ensemble generated by MD simulations showed that only α-amino acid containing ligands (**1**, **2**, **3**, **5**, **6**, **7** and **10**) are capable of adopting bent, folded structures both in H_2O and DMSO (Table 2). Various types of γ- and β-turns were identified along the

Table 2
Frequency of different secondary structures expressed as percentages of the total conformational ensemble, generated by molecular dynamics for ligands with native α-peptide backbone.

	Ligand		γ-Turn location and type						β-Turn type						
			1–3		2–4		3–5								
			Classic	Inverse	Classic	Inverse	Classic	Inverse	I	I′	II	II′	III	IV	VIII
H_2O	**1**	*cis*[a]	–	–	–	<0.50	–	<0.50	<0.50	–	<0.50	–	–	2.21	<0.50
		trans	–	3.20	<0.50	<0.50	<0.50	<0.50	0.99	–	4.96	–	5.16	6.74	<0.50
	2	*cis*	–	–	<0.50	<0.50	<0.50	<0.50	<0.50	–	<0.50	–	–	5.12	<0.50
		trans	–	2.26	0.68	<0.50	–	<0.50	25.88	–	–	–	9.06	8.45	<0.50
	3		7.67	<0.50	–	–	17.78	3.31	–	<0.50	–	<0.50	–	13.41	<0.50
	5	*cis*	–	–	–	<0.50	<0.50	<0.50	0.64	–	<0.50	–	–	4.06	<0.50
		trans	–	1.32	–	<0.50	<0.50	<0.50	29.14	–	–	–	<0.50	15.96	<0.50
	6		–	–	<0.50	8.12	<0.50	0.54	–	–	8.63	–	–	54.83	–
	7	*cis*	–	–	–	–	–	<0.50	–	–	–	–	–	2.77	0.52
		trans	–	4.38	–	–	–	<0.50	<0.50	–	–	–	–	1.42	0.80
	10		–	–	1.75	7.92	0.65	0.61	0.90	–	<0.50	<0.50	<0.50	28.63	<0.50
DMSO	**1**	*cis*[a]	–	–	<0.50	<0.50	–	<0.50	1.83	–	<0.50	–	–	15.80	–
		trans	–	5.90	0.55	1.29	–	<0.50	2.17	–	14.18	–	2.67	19.34	–
	2	*cis*	–	–	8.60	<0.50	<0.50	<0.50	–	–	<0.50	–	–	6.23	–
		trans	–	0.55	–	<0.50	–	<0.50	22.92	–	–	–	1.79	19.31	<0.50
	3		2.88	–	–	–	18.73	12.13	–	<0.50	–	<0.50	–	17.72	–
	5	*cis*	–	–	–	<0.50	<0.50	<0.50	<0.50	–	<0.50	–	–	4.70	–
		trans	–	0.72	–	–	<0.50	<0.50	41.14	–	–	–	<0.50	15.11	–
	6		–	–	0.54	9.36	<0.50	0.68	–	–	12.30	–	<0.50	50.09	–
	7	*cis*	–	–	–	–	–	1.27	<0.50	–	–	–	–	2.77	<0.50
		trans	–	2.24	–	–	–	1.02	–	–	<0.50	–	–	3.85	<0.50
	10		–	–	4.42	2.75	4.36	0.73	<0.50	–	<0.50	2.74	<0.50	39.51	<0.50

[a] Configuration of the Tyr^1–Pro^2 peptide bond.

Table 3
Specific structural properties of compounds **1–10** obtained from MD simulations.

			1		**2**		**3**	**4**	**5**		**6**	**7**		**8**	**9**	**10**
			c[a]	*t*	*c*	*t*			*c*	*t*		*c*	*t*			
H_2O	Occurrence of specific intramolecular hydrogen bonds/%	CO(1)–HN(3)	0.0	7.2	0.0	17.3	25.5	1.3	0.0	12.9	–	0.0	28.8	6.5	1.3	–
		CO(2)–HN(4)	10.2	9.0	7.6	8.0	37.6	12.5	9.0	3.3	76.7	–	–	30.2	5.7	56.2
		CO(1)–HN(4)	0.0	10.6	0.0	36.7	–	1.4	0.0	32.2	31.9	–	–	13.1	3.6	3.1
		CO(2)–H_2N(C-term.)	14.0	31.8	16.7	15.5	4.3	4.3	1.3	1.3	1.4	0.0	0.0	16.7	22.2	2.0
		CO(1)–H_2N(C-term.)	0.9	4.4	0.0	23.5	2.1	5.9	0.0	9.2	55.6	0.0	0.0	25.6	3.0	4.7
		NH_3^+(1)–OC(3)	1.2	0.0	0.3	0.0	0.8	12.3	10.3	0.0	0.0	50.8	0.0	0.0	9.6	0.0
		NH_3^+(1)–OC(4)	4.7	0.0	4.9	3.5	0.5	6.1	27.8	21.1	0.3	0.0	0.0	0.3	0.7	0.0
	Occurrence of bent structure[b]/%		26.6	18.4	8.9	45.4	22.4	73.1	39.1	48.8	64.1	43.1	22.6	31.9	23.3	30.6
	Pharmacophore distances[c]/%		2.3	4.8	13.7	5.7	1.2	3.1	2.8	5.6	1.3	8.3	1.2	0.5	4.5	3.2
DMSO	Occurrence of specific intramolecular hydrogen bonds/%	CO(1)–HN(3)	0.0	9.4	0.0	10.1	9.7	3.5	0.0	8.7	–	0.0	3.8	4.4	3.2	–
		CO(2)–HN(4)	12.6	37.8	21.9	0.8	57.9	25.5	5.0	1.1	64.9	–	–	10.2	19.3	50.7
		CO(1)–HN(4)	0.0	11.5	0.0	18.2	–	0.0	0.0	33.6	34.4	–	–	0.0	0.2	9.3
		CO(2)–H_2N(C-term.)	10.9	21.3	12.2	2.5	2.4	17.7	3.9	0.5	2.0	7.9	29.1	15.4	33.1	2.0
		CO(1)–H_2N(C-term.)	0.0	23.7	0.0	1.7	0.2	0.0	0.0	15.8	34.5	0.0	0.0	0.0	0.6	6.3
		NH_3^+(1)–OC(3)	0.0	0.0	0.0	2.0	1.0	33.1	0.9	0.0	0.0	24.7	0.0	0.0	13.3	0.0
		NH_3^+(1)–OC(4)	5.2	2.4	0.1	54.7	<0.1	47.5	36.9	24.7	14.9	0.9	0.0	0.0	11.9	4.5
	Occurrence of bent structure[b]/%		36.8	39.3	6.9	66.3	20.3	57.8	40.8	60.7	63.3	30.6	13.5	0.1	8.3	44.7
	Pharmacophore distances[c]/%		17.3	2.8	25.5	14.9	0.7	<0.1	3.3	21.9	2.8	17.5	8.7	1.6	7.9	22.4

[a] Configuration of the Tyr^1–Pro^2 peptide bond.
[b] Bent structure was assigned based on the analysis of the N(1)-C_α(2)-C_α(3)-C(4) virtual dihedral angle and the distance between the terminal C_α-atoms.
[c] Occurrence of structures in which all pharmacophore distances are in the correct range according to Yamazaki et al. [37].

trajectories. Classic secondary structural definitions do not apply to β-amino acid containing peptides (**4**, **8** and **9**). Therefore those ligands were compared to each other and to α-peptides based on the occurrence of specific intramolecular hydrogen bonds and their backbone curvature measured through the N(1)-C_α(2)-C_α(3)-C(4) virtual dihedral angle and the distance between terminal C_α-atoms [72]. The overall occurrence of bent structures (Table 3) was found to be relatively high for most ligands, both in H_2O and DMSO compared to other peptides of this size [74]. For peptides with a native backbone, populations of structures defined by specific hydrogen bonds (Table 3) are in good agreement with populations obtained from STRIDE analysis, despite the fact that STRIDE assigns secondary structure based on backbone torsional angles rather than hydrogen bonds and this generally leads to a more frequent recognition of turn structures [74]. Hydrogen bond analysis also confirmed the occurrence of various γ- and β-turn structures for α-peptides (Fig. 3.) and helped to identify analogous conformational elements of β-amino acid containing peptides shown on Fig. 4.

3.2. Side-chain conformations

Analysis of side-chain rotamer populations revealed that the *trans* conformation of the χ^1 dihedral angle of the Tyr^1 side chain is

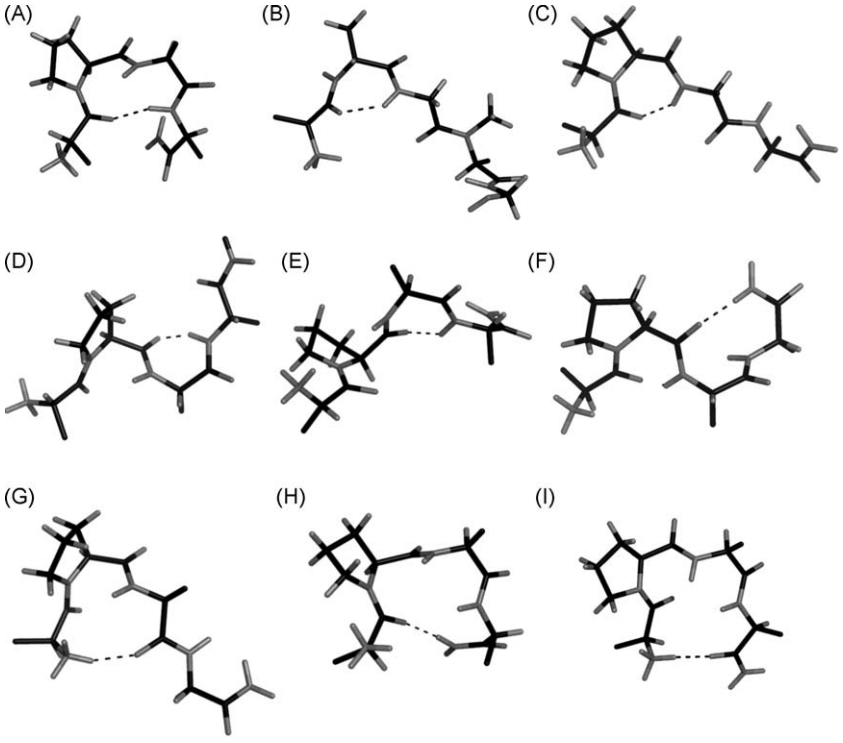

Fig. 3. Folded structures identified by the analysis of specific intramolecular hydrogen bonds for α- peptides. (A) β-turn, (B, D) classic γ-turn, (C, E) inverse γ-turn, (F) C-terminal β-turn, (G) N-terminal C_{11}-loop, (H) C-terminal C_{13}-loop, (J) N to C-terminal loop.

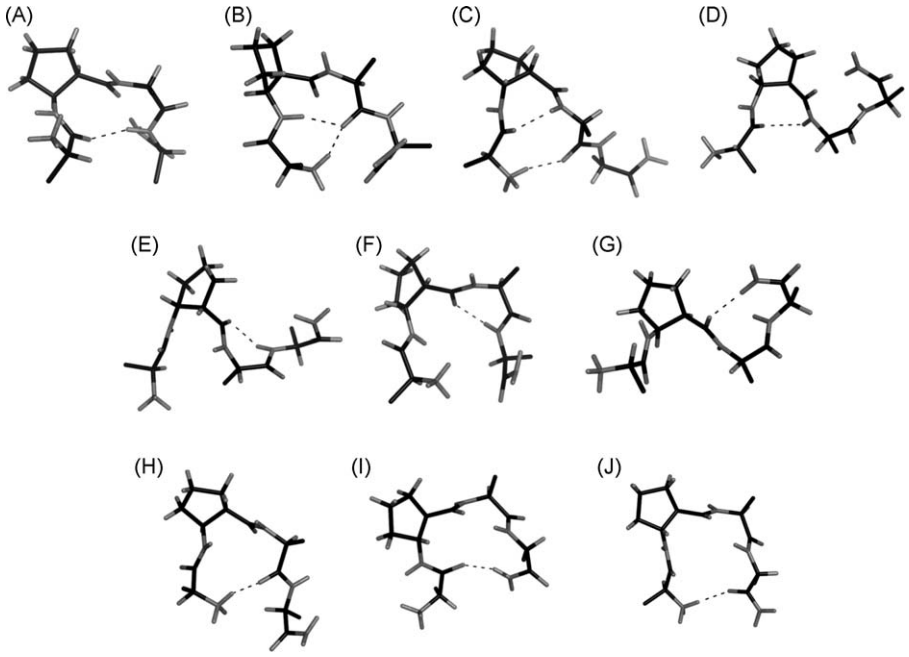

Fig. 4. Folded structures identified by the analysis of specific hydrogen bonds for β-amino acid containing peptides. (A) C_{11}-turn, (B) C_9-turn, (C) "classic" C_8-turn, (D) "inverse" C_8-turn, (E) classic γ-turn, (F) inverse γ-turn, (G) C-terminal β-turn, (H) N-terminal C_{12}-loop, (I) C-terminal C_{14}-loop, (J) N to C-terminal loop.

highly favored for all peptides both in H_2O and in DMSO (Table 4). In DMSO the preference for the *gauche*− conformation of χ^1 of the aromatic side chain in the third position and the flexibility of the 4th aromatic side chain [39] was found to be slightly higher in ligands with higher MOR affinity. In H_2O, these latter trends were less apparent or were not observed at all.

3.3. Pharmacophore distances

The fraction of the conformational ensemble in which previously proposed criteria for the distances between pharmacophore groups [37] are fulfilled were also determined for all ligands in both solvents (Table 3). In H_2O these fractions were found to be relatively small for all peptides, including morphiceptin, the prototype of this bioactive structure model and distance requirements. In DMSO these fractions were significantly higher for **1**, **2**, **5**, **7** and **10**.

3.4. Structure–activity relationships

The ratio between the number of molecules studied here (the training set) and the number of structural descriptors is too low for the safe application of robust statistical methods. Furthermore, due to the structural diversity of the ligand set with regard to the structural parameters in question, traditional QSAR methods would not provide reliable models. Therefore, the aforementioned structural parameters were evaluated simultaneously through the transformation of the numeric data in Tables 3 and 4 into a graphical representation with the application of the following guidelines. MOR affinities and the magnitude of how well each ligand conforms to the four structural criteria were presented on a three-level scale. High, moderate and low receptor affinities were assigned appropriately according to the value ranges listed in Table 1. For structural parameters, their maximal and minimal populations observed throughout the whole data were considered

Table 4
Side-chain rotamer populations of compounds **1–10** expressed as percentages of the total conformational ensemble, generated by molecular dynamics.

			1		**2**		**3**	**4**	**5**		**6**	**7**		**8**	**9**	**10**
			c	t	c	t			c	t		c	t			
H_2O	Tyr[1]	*g*+	2.2	7.2	1.8	5.3	9.7	1.3	1.3	11.1	11.0	3.6	7.3	3.4	10.4	13.5
		g−	5.3	14.1	2.7	15.5	17.5	41.8	1.4	28.3	17.0	5.3	16.3	2.9	18.9	5.4
		t	92.5	78.7	95.5	79.2	72.8	56.9	97.3	60.5	72.0	91.1	76.4	93.7	70.7	81.4
	Trp[3]/Phe[3]	*g*+	26.8	42.2	27.1	14.0	–	4.0	29.1	60.4	0.0	15.4	10.7	4.6	6.4	0.0
		g−	68.0	31.0	17.2	33.2	–	6.8	64.7	30.9	0.0	40.6	47.1	47.2	10.8	0.0
		t	5.2	26.8	55.7	52.8	–	89.2	6.2	8.6	0.0	44.0	42.2	48.2	82.8	0.0
	Phe[4]/N-Me-Phe[4]	*g*+	36.8	48.9	40.0	33.6	0.0	3.6	–		2.9	–		7.6	13.8	3.2
		g−	38.0	32.2	41.8	36.5	40.2	6.6	–		37.7	–		18.5	7.1	7.5
		t	25.2	18.9	18.2	29.9	59.7	89.8	–		59.4	–		73.9	79.1	89.3
DMSO	Tyr[1]	*g*+	4.2	33.2	5.5	14.2	0.2	8.5	0.5	6.1	36.8	0.2	17.3	3.4	3.8	25.7
		g−	2.0	7.1	2.1	12.1	29.3	69.0	0.1	10.9	17.6	4.4	8.2	15.5	11.5	18.1
		t	93.8	59.7	92.4	73.7	70.5	22.5	99.4	83.0	45.7	95.4	74.5	81.1	84.7	56.2
	Trp[3]/Phe[3]	*g*+	15.8	20.2	40.2	27.0	–	4.4	10.3	36.3	–	14.3	16.5	3.5	5.1	–
		g−	70.3	47.0	14.7	41.4	–	8.0	81.6	47.8	–	32.2	37.6	40.7	2.4	–
		t	13.9	32.8	45.1	31.6	–	87.6	8.1	15.9	–	53.5	45.9	55.8	92.5	–
	Phe[4]/*N*-Me-Phe[4]	*g*+	37.6	43.8	39.5	33.6	13.0	15.3	–		16.4	–		0.2	20.5	4.6
		g−	28.0	24.3	20.8	12.1	42.7	21.8	–		20.5	–		3.6	12.3	5.7
		t	34.4	31.9	39.7	54.3	44.3	62.9	–		63.1	–		96.2	67.2	89.7

for such assignments. Thus, the predominance of *trans* conformation of the χ^1 dihedral angle of the Tyr^1 side chain was assigned if the population of that conformational state was higher that 66%. Consequently moderate dominance was assigned when this population was between 33% and 66% and populations below 33% were not considered as dominant. Taking into account that the flexibility of side chains increases from the N- to the C-terminus, transformation criteria were less strict for the conformation of the aromatic side chain in the third position of the sequences. The occurrence of the *gauche*− conformation was assigned to be low if the population of that conformational state was below 10%, moderate if it was between 10% and 33% and high above 33%. Flexibility of the aromatic side chain in the fourth position was classified to be high if the populations of all three conformational states of that side chain were above 10%. If the population of one conformational state was below 10% then moderate flexibility was assigned and if there was only one conformational state present with a population above 10%, then flexibility was rated low. Similarly, occurrence of bent backbone structure was considered high over 30% of the ensemble, moderate between 10% and 30% and low below 10%. For ligands in which *cis*–*trans* isomerization of the Tyr^1–Pro^2 peptide bond occurs, data obtained for the *cis* and *trans* stereoisomers were weighted by 0.3 and 0.7, respectively to reflect their population ratio in solution [37,41,75]. Because of the high structural diversity of ligands studied here, special arbitrary assignments were necessarily done in the following four cases. Ligand 3 has only two aromatic side chains, one in position 1 and one in position 4. Since the role of the side chain in position 4 is ambiguous and it may act as the side chain in position 3 in other peptides, occurrence of the *gauche*− conformation of the (missing) third side chain was assigned based on the properties of the side chain in the fourth position. Similarly, ligands 5 and 7 do not have an aromatic side chain in position 4. A missing side chain may be advantageous in binding, because the possibility of steric hindrance is lower. On the other hand, this may also result in a lower absolute value of binding free energy because of lost contacts between the bound ligand and the receptor. As a result of these considerations, moderate flexibility was assigned to the (missing) fourth aromatic side chains of **5** and **7**. The third aromatic side chains of **6** and **10** are conformationally constrained. Fig. 5A and B show the possible orientations of the aromatic moiety of (*R*)-spiro-Aba-Gly and (*S*)-Aba-Gly, respectively. For (*R*)-spiro-Aba-Gly a region close to that of the *gauche*− conformation is occupied by the conformer depicted in gray. Since no significant preference for this conformer over the other conformer (Fig. 5A, black) was observed, the occurrence of the *gauche*− conformation of the third aromatic side chain of **6** was rated moderate. For (*S*)-Aba-Gly none of the depicted conformers occupy the *gauche*− region, thus the occurrence of the *gauche*− conformation of the third aromatic side chain was classified as low for ligand **10**. The conformation of the first and the third aromatic side chain of ligand **4** were found to be predominantly *gauche*− and *trans*, respectively. This specific, simultaneous deviation suggests that the optimal relative orientation of pharmacophores is furnished by a different combination of side chain and backbone conformations for this peptide. Accordingly, corresponding structural requirements were considered fulfilled for this peptide in DMSO. In H_2O the predominance of the *gauche*− conformation of Tyr^1 of ligand **4** was less pronounced, therefore it was classified as moderate. The resultant graphical representation shows correlation between biological data and structural data obtained from simulations in DMSO (Table 5), suggesting that the structural model proposed here is reasonable. No correlation is apparent for data obtained in aqueous environment.

3.5. Receptor–ligand complex models

Structures which conform to the above mentioned criteria were extracted from the trajectory of ligand **2** in order to compare them with existing pharmacophore models. Representatives of these structures (Fig. 6A) show that the four parameters investigated in this study do not define a rigid model. These representative structures of **2** were found to fit well in the putative binding site of a previously proposed MOR–ligand complex model [54] having the aromatic side chains aligned to the corresponding side chains of JOM6, the original ligand of the model. Fig. 6B shows an energy minimized complex of the MOR and **2** and JOM6 is overlaid for comparison. Most of the contacts formed between JOM6 and the MOR are maintained by **2** and an additional hydrophobic contact is formed between Pro^2 of **2** and Ile^{322} of the MOR. Furthermore, Phe^4

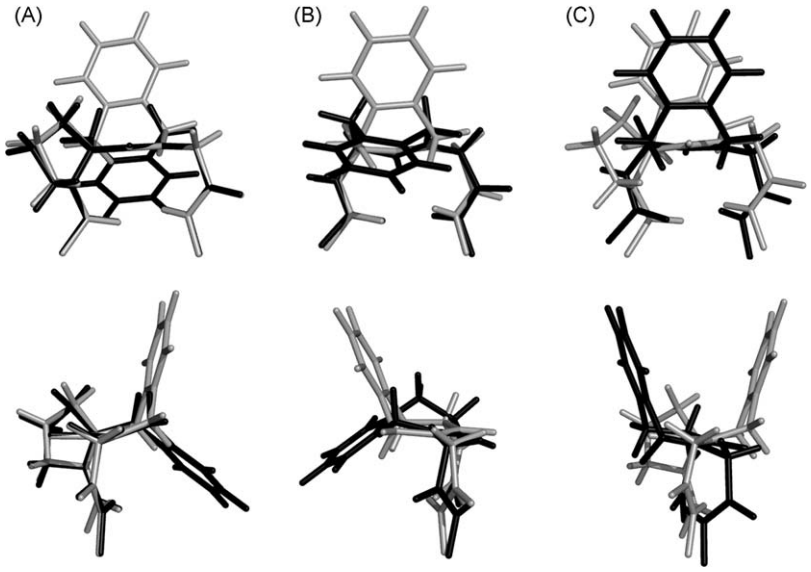

Fig. 5. Structural properties of the studied pseudo-dipeptides. (A) Possible spatial orientations of the benzazepinone ring in Ac-(*R*)-spiro-Aba-Gly-NMe in bent backbone conformation viewed from the front (upper panel) and from the side (lower panel). (B) Possible spatial orientations of the benzazepinone ring in Ac-(*S*)-Aba-Gly-NMe in bent backbone conformation viewed from the front (upper panel) and from the side (lower panel). (C) Spatial orientation of the benzazepinone ring in Ac-(*R*)-spiro-Aba-Gly-NMe and Ac-(*S*)-Aba-Gly-NMe, viewed from the front (upper panel) and from the side (lower panel).

Table 5
Graphical representation of the conformity of the obtained structural parameters to the proposed criteria of μ-opioid activity.

		1	2	3	4	5	6	7	8	9	10
H_2O	$\chi^1(1) = t$										
	$\chi^1(3) = g-$										
	$\chi^1(4)$ flexible										
	bent backbone										
		1	2	3	4	5	6	7	8	9	10
DMSO	$\chi^1(1) = t$										
	$\chi^1(3) = g-$										
	$\chi^1(4)$ flexible										
	bent backbone										
	receptor affinity										

Colors represent the following classifications: blank background = high, gray = moderate, black = low. See text for detailed explanation. Numbers in parentheses reflect the position of the corresponding side chain in the sequence.

of **2** is packed in a tight hydrophobic cluster with Tyr^{148}, Val^{202} and Val^{236} of the receptor. In this conformation of **2** the distances between the three pharmacophore groups are 7.9, 7.2 and 12.6 Å, respectively. See the Supporting Info for further complexes between the MOR and **2**.

4. Discussion

4.1. Degree of conformational sampling

To reasonably reach as high a degree of conformational sampling as possible, three separate MD simulations were run, starting from different structures. The main accessible conformational states, identified as described in the Methods section, were used as starting structures. Secondary structure analysis and comparison of the separate 50 ns long trajectories revealed, that for most compounds, results depend on the starting structure. (See Supplementary Info) This trend is even more pronounced for simulations performed in DMSO, possibly due to the higher viscosity of this solvent resulting in slower conformational transition rates. These observations justify the approach taken here, as a significant increase in the degree of conformational sampling was achieved through parallel simulations, starting from different structures. Data in Table 2 displays a high number of visited structural states which suggests that the conformational space was explored adequately.

4.2. Secondary structure

The occurrence of γ- and β-turn structures of the studied compounds in H_2O and DMSO is in agreement with previous

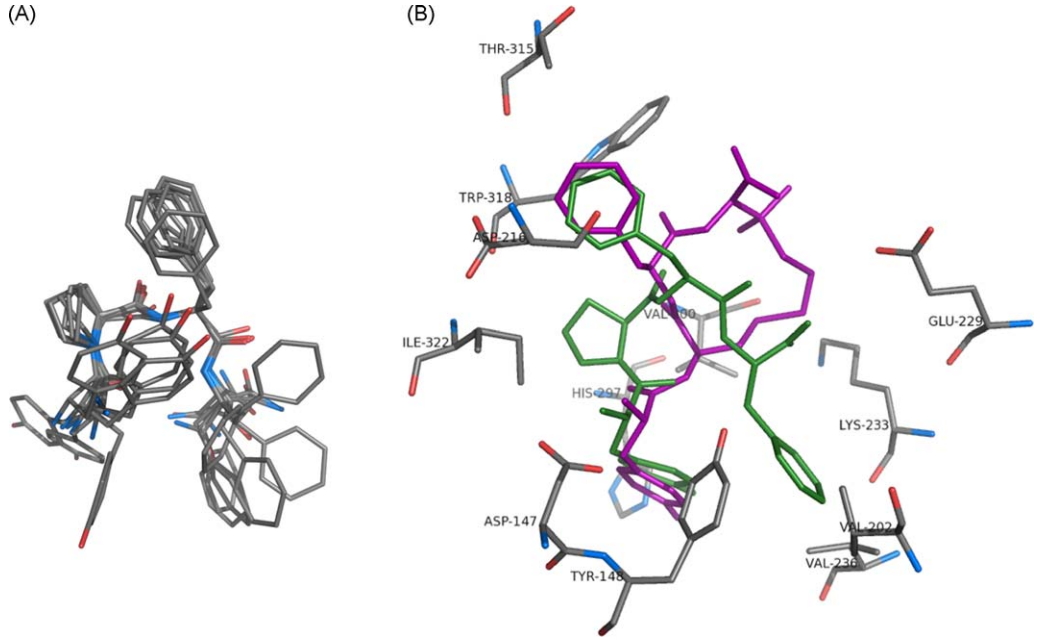

Fig. 6. (A) Structures of **2** with the desired structural parameters in regard of MOR binding. (B) Spatial orientation of **2** with all four structural criteria fulfilled (green) and JOM6 (magenta) in the putative binding cavity of the MOR. Hydrogen atoms are omitted for clarity.

observations [29,40,60]. However, no specific structural state was found which could be related to MOR affinity based on its frequency. Similarly, populations of structures defined by specific intramolecular hydrogen bonds did not show direct correlation with biological data, neither in H_2O nor in DMSO. Even if we assume that receptor binding conditions are approximated correctly by the simulation conditions, the results prove that there are more parameters than just the backbone conformation which should be taken into account. However, this does not rule out the role and importance of one or more specific backbone conformational states. The high population of bent structures in comparison with previous observations for peptides of this size [74] supports the hypothesis that a bent backbone structure is at least partially responsible for binding to the MOR [25,26,32,39].

4.3. Side-chain conformations

The importance of the *trans* conformation of the Tyr^1 side chain was recognized in agreement with literature data [38,46], for all peptides except compound **4**. However, for that peptide simultaneous deviations were found compared to the structural trends observed for the rest of the ligand pool, promoting the idea that more than just one binding mode of MOR ligands is possible. The preference for the *gauche*− conformation of the aromatic side chain in the third position and the flexibility of the C-terminal aromatic moiety, observed for high affinity ligands during simulations performed in DMSO supports the structural model proposed on the basis of the structure of cyclic somatostatin analogues [39]. In H_2O these latter trends were less apparent or were not observed at all. The presence of a C-terminal aromatic residue is not essential for MOR binding since some ligands, such as **5** and **7**, display considerable binding affinity despite the lack of this side chain. Nevertheless, the presence of an aromatic side chain may enhance affinity by forming hydrophobic contacts with the corresponding part of the MOR. In an earlier study the preference for the *gauche*− conformation of the C-terminal aromatic side chain of EM-2 was indicated [24]. The demand for flexibility observed in the present study does not argue against this previous proposal but rather suggests that this preference may differ from ligand to ligand. Furthermore, the binding pocket for this residue may be more rigid than other regions of the active site and the ligands may have to possess considerable adaptability in order to fit in.

4.4. Pharmacophore distances

The ligands studied here did not conform to the previously proposed bioactive structural model [37] in which the spatial orientation of pharmacophores is defined by their relative distances. The very low population of structures which fulfill these distance requirements suggests that, either the receptor-bound structure of these peptides is not favored in H_2O, or this previously introduced structural model is not generally applicable. Some ligands displayed higher populations of the correct structure in DMSO, although this trend did not reflect the biological properties. This leads to the assumption that re-evaluation of this previous model is needed, or at least more that just one binding mode has to be considered.

4.5. Structure–activity relationships

In summary, the following four parameters were confirmed as potential conformational requirements of MOR activity: 1. *trans* conformation of the χ^1 torsional angle of Tyr^1, 2. *gauche*− conformation of the χ^1 torsional angle of the aromatic side chain in the third position of the sequence, 3. flexibility of the C-terminal aromatic side chain, 4. bent backbone structure. However, none of these parameters are exclusive determinants of bioactivity and deviation from their optimal state may still result in significant MOR affinity as long as the other requirements are fulfilled. This is not just acceptable but also expected since similar spatial orientation of pharmacophores may result from various backbone- and side-chain conformations. It is apparent that deviation from bent backbone structure and decreased flexibility of the C-terminal aromatic side chain are more tolerated, while the conformation of the first and the third aromatic side chains have a more dramatic impact on biological activity. Nevertheless, quantitative statements about the exact contribution of each parameter to the bioactive conformation cannot be given on the basis of the work presented here.

4.6. Comparison with existing models

The only difference between the set of parameters presented here and those proposed earlier on the basis of cyclic somatostatin analogues [39] is that the *trans* conformation of the corresponding Tyr side chain was found to be dominant instead of *gauche*+. However, the spatial position of that side chain depends not only on χ^1, but also on the Ψ dihedral angle of Tyr^1 as shown in Fig. 6A. Similar spatial orientation can be achieved through different combinations of χ^1 and Ψ angle values. Our proposed conformation fits well in the binding cavity of a previously proposed MOR–ligand complex model [54] as shown by the example in Fig. 6B. Even the distances between the three pharmacophore groups were found to be in perfect agreement with those previously proposed by Yamazaki et al. [37], despite the exclusive importance of those parameters not being confirmed by our analysis (Table 3). More intermolecular contacts were found between the MOR and **2** in comparison with the case of JOM6, the ligand presented in the model of Mosberg [54]. This indicates the possibility of a stronger interaction between the MOR and **2** compared to the MOR and JOM6, which results different binding affinities of these ligands [7,54]. Nevertheless, results presented here indicate that the example shown on Fig. 6B is not an ultimate pharmacophore model and that not just one but more binding modes are possible. Furthermore, previously discussed concerns about the exact location of the binding site make this picture look more complicated. This may explain the difference between the model presented here and the previously proposed model obtained from QSAR studies [43] and the diversity of previous assumptions about structure–activity relationships of MOR ligands.

5. Conclusions

Results of MD simulations performed in DMSO revealed a correlation between MOR affinity and the simultaneous fulfillment of four structural criteria (Table 5). Such correlation was not observed for data obtained from aqueous simulations. H_2O and DMSO are no substitute for biological environments, but their macroscopic physical properties, especially those of DMSO, are very similar. Still, general discretion is advised for their application and interpretation of results. Our results demonstrate that DMSO may be a better approximation to the mechanical and electrostatic environment of binding to the MOR than H_2O.

The four criteria confirmed in this study are not sufficient to define a rigid structure exclusively associated with bioactivity and the quantitative contribution of each parameter is yet unknown. However, information obtained here could possibly resolve many contradictions in the past literature of opioid peptides and may help to identify possible structural candidates in the design of novel MOR agonists.

Acknowledgments

This work was supported by Hungarian OTKA PD-73081 and European LSHC-CT-2006-037733 "NORMOLIFE" grants.

Appendix A. Supplementary data

Supplementary data associated with this article can be found, in the online version, at doi:10.1016/j.jmgm.2009.11.006.

References

[1] W.R. Martin, C.G. Eades, J.A. Thompson, R.E. Huppler, P.E. Gilbert, The effects of morphine- and nalorphine-like drugs in the nondependent and morphine-dependent chronic spinal dog, J. Pharmacol. Exp. Ther. 197 (1976) 517–532.
[2] L.A. Lord, A.A. Waterfield, J. Hughes, H.W. Kosterlitz, Endogenous opioid peptides: multiple agonist and receptors, Nature 267 (1977) 495–499.
[3] Y. Chen, A. Mestek, J. Liu, J.A. Hurley, L. Yu, Molecular cloning and functional expression of a mu-opioid receptor from rat brain, Mol. Pharmacol. 44 (1993) 8–12.
[4] K. Fukuda, S. Kato, K. Mori, M. Nishi, H. Takeshima, Primary structures and expression from cDNAs of rat opioid receptor delta- and mu-subtypes, FEBS Lett. 327 (1993) 311–314.
[5] R.C. Thompson, A. Mansour, H. Akil, S.J. Watson, Cloning and pharmacological characterization of a rat mu opioid receptor, Neuron 11 (1993) 903–913.
[6] R. Przewłocki, B. Przewłocka, Opioids in chronic pain, Eur. J. Pharmacol. 429 (2001) 79–91.
[7] J.E. Zadina, L. Hackler, L.J. Ge, A.J. Kastin, A potent and selective endogenous agonist for the mu-opiate receptor, Nature 386 (1997) 499–502.
[8] B.K. Handa, A.C. Land, J.A. Lord, B.A. Morgan, M.J. Rance, C.F. Smith, Analogues of beta-LPH61-64 possessing selective agonist activity at mu-opiate receptors, Eur. J. Pharmacol. 70 (1981) 531–540.
[9] K.J. Chang, A. Lillian, E. Hazum, Cuatrecasas, J.K. Chang, Morphiceptin, (NH4-Tyr-Pro-Phe-Pro-CONH2): a potent and specific agonist for morphine (mu) receptors, Science 212 (1981) 75–77.
[10] J.T. Pelton, K. Gulya, V.J. Hruby, S.P. Duckles, H.I. Yamamura, Conformationally restricted analogs of somatostatin with high μ-opiate receptor specificity, Proc. Natl. Acad. Sci. U.S.A. 88 (1985) 236–239.
[11] V.J. Hruby, R.S. Agnes, Conformation-activity relationships of opioid peptides with selective activities at opioid receptors, Biopolymers 51 (1999) 391–410.
[12] W. Pan, A.J. Kastin, From MIF-1 to endomorphin: the Tyr-MIF-1 family of peptides, Peptides 28 (2007) 2411–2434.
[13] J. Érchegyi, A.J. Kastin, J.E. Zadina, Isolation of a novel tetrapeptide with opiate and antiopiate activity from human brain cortex: Tyr-Pro-Trp-Gly-NH_2 (Tyr-W-MIF-1), Peptides 13 (1992) 623–631.
[14] A. Sugimoto-Watanabe, K. Kubota, K. Fujibayashi, K. Saito, Antinociceptive effect and enzymatic degradation of endomorphin-1 in newborn rat spinal cord, Jpn. J. Pharmacol. 81 (1999) 264–270.
[15] G. Cardillo, L. Gentilucci, P. Melchiorre, S. Spampinato, Synthesis and binding activity of endomorphin-1 analogues containing beta-amino acids, Bioorg. Med. Chem. Lett. 10 (2000) 2755–2758.
[16] M. Keller, C. Boissard, L. Patiny, N.N. Chung, C. Lemieux, M. Mutter, P.W. Schiller, Pseudoproline-containing analogues of morphiceptin and endomorphin-2: evidence for a cis Tyr-Pro amide bond in the bioactive conformation, J. Med. Chem. 44 (2001) 3896–3903.
[17] I. Lengyel, G. Orosz, D. Biyashev, L. Kocsis, M. Al-Khrasani, A. Rónai, Cs. Tömböly, Zs. Fürst, G. Tóth, A. Borsodi, Side chain modifications change the binding and agonist properties of endomorphin 2, Biochem. Biophys. Res. Commun. 290 (2002) 153–161.
[18] G. Cardillo, L. Gentilucci, A.R. Qasem, F. Sgarzi, S. Spampinato, Endomorphin-1 analogues containing beta-proline are mu-opioid receptor agonists and display enhanced enzymatic hydrolysis resistance, J. Med. Chem. 45 (2002) 2571–2578.
[19] M. Doi, A. Asano, E. Komura, Y. Ueda, The structure of an endomorphin analogue incorporating 1-aminocyclohexane-1-carboxlylic acid for proline is similar to the beta-turn of Leu-enkephalin, Biochem. Biophys. Res. Commun. 297 (2002) 138–142.
[20] S.D. Bryant, Y. Jinsmaa, S. Salvadori, Y. Okada, L.H. Lazarus, Dmt and opioid peptides: a potent alliance, Biopolymers 71 (2003) 86–102.
[21] R. Kruszynski, J. Fichna, J.-C. do-Rego, T. Janecki, P. Kosson, W. Pakulska, J. Costentin, A. Janecka, Novel endomorphin-2 analogs with mu-opioid receptor antagonist activity, Bioorg. Med. Chem. 13 (2005) 6713–6717.
[22] T. Li, Y. Fujita, Y. Tsuda, A. Miyazaki, A. Ambo, Y. Sasaki, Y. Jinsmaa, S.D. Bryant, L.H. Lazarus, Y. Okada, Development of potent mu-opioid receptor ligands using unique tyrosine analogues of endomorphin-2, J. Med. Chem. 48 (2005) 586–592.
[23] E. Sperlinga, P. Kosson, Z. Urbanczyk-Lipkowska, G. Ronsisvalle, D.B. Carr, A.W. Lipkowski, 6-Hydroxy-1,2,3,4-tetrahydro-isoquinoline-3-carboxylic acid mimics active conformation of tyrosine in opioid peptides, Bioorg. Med. Chem. Lett. 15 (2005) 2467–2469.
[24] Cs. Tömböly, K.E. Kövér, A. Péter, D. Tourwé, D. Biyashev, S. Benyhe, A. Borsodi, M. Al-Khrasani, A. Rónai, G. Tóth, Structure-activity study on the Phe side chain arrangement of endomorphins using conformationally constrained analogues, J. Med. Chem. 47 (2004) 735–743.
[25] A. Keresztes, M. Szűcs, A. Borics, K.E. Kövér, E. Forró, F. Fülöp, Cs. Tömböly, A. Péter, A. Páhi, G. Fábián, M. Murányi, G. Tóth, New endomorphin analogues containing alicyclic beta-amino acids: influence on bioactive conformation and pharmacological profile, J. Med. Chem. 51 (2008) 4270–4279.
[26] Cs. Tömböly, S. Ballet, D. Feytens, K.E. Kövér, A. Borics, S. Lovas, M. Al-Khrasani, Z. Fürst, G. Tóth, S. Benyhe, D. Tourwé, Endomorphin-2 with a beta-turn backbone constraint retains the potent mu-opioid receptor agonist properties, J. Med. Chem. 51 (2008) 173–177.
[27] G. Cardillo, L. Gentilucci, A. Tolomelli, R. Spinosa, M. Calienni, A.R. Qasem, S. Spampinato, Synthesis and evaluation of the affinity toward mu-opioid receptors of atypical, lipophilic ligands based on the sequence c[-Tyr-Pro-Trp-Phe-Gly-], J. Med. Chem. 47 (2004) 5198–5203.
[28] A. Janecka, J. Fichna, R. Kruszynski, Y. Sasaki, A. Ambo, J. Costentin, J.-C. Do-Rego, Synthesis and antinociceptive activity of cyclic endomorphin-2 and morphiceptin analogs, Biochem. Pharm. 71 (2005) 188–195.
[29] A. Janecka, R. Kruszynski, Conformationally restricted peptides as tools in opioid receptor studies, Curr. Med. Chem. 12 (2005) 471–481.
[30] Q.-Y. Zhao, Q. Chen, D.-J. Yang, Y. Feng, Y. Long, P. Wang, R. Wang, Endomorphin 1[psi] and endomorphin 2[psi], endomorphins analogues containing a reduced (CH_2NH) amide bond between Tyr^1 and Pro^2, display partial agonist potency but significant antinociception, Life Sci. 77 (2005) 1155–1165.
[31] Y. Okada, A. Fukumizu, M. Takahashi, Y. Shimizu, Y. Tsuda, T. Yokoi, S.D. Bryant, L.H. Lazarus, Synthesis of stereoisomeric analogues of endomorphin-2, H-Tyr-Pro-Phe-Phe-NH_2, and examination of their opioid receptor binding activities and solution conformation, Biochem. Biophys. Res. Commun. 276 (2000) 7–11.
[32] M. Eguchi, R.Y.W. Shen, J.P. Shea, M.S. Lee, M. Kahn, Design, synthesis, and evaluation of opioid analogues with non-peptidic beta-turn scaffold: enkephalin and endomorphin mimetics, J. Med. Chem. 45 (2002) 1395–1398.
[33] B.A. Harrison, T.M. Gierasch, C. Neilan, G.W. Pasternak, G.L. Verdine, High-affinity mu opioid receptor ligands discovered by the screening of an exhaustively stereodiversified library of 1,5-enediols, J. Am. Chem. Soc. 124 (2002) 13352–13353.
[34] B.A. Harrison, G.W. Pasternak, G.L. Verdine, 2,6-Dimethyltyrosine analogues of a stereodiversified ligand library: highly potent, selective, non-peptidic mu opioid receptor agonists, J. Med. Chem. 46 (2003) 677–680.
[35] R. Schwyzer, Prediction of potency and receptor selectivity of regulatory peptides: the membrane compartment concept, in: D. Theodoropoulos (Ed.), Peptides, vol. 86, de Gruyter, Berlin, 1987, pp. 7–23.
[36] A.F. Casy, The Steric Factor in Medicinal Chemsitry: Dissymetric Probes of Pharmacological Receptors, Plenum Press, New York, 1993.
[37] T. Yamazaki, S. Ro, M. Goodman, N.N. Chung, P.W. Schiller, A topochemical approach to explain morphiceptin bioactivity, J. Med. Chem. 36 (1993) 708–719.
[38] M.G. Paterlini, F. Avitable, B.G. Ostrowski, D.M. Ferguson, P.S. Portoghese, Stereochemical requirements for receptor recognition of the μ-opioid peptide endomorphin-1, Biophys. J. 78 (2000) 590–599.
[39] W.M. Kazmierski, R.D. Ferguson, A.W. Lipkowski, V.J. Hruby, A topographical model of mu-opioid and brain somatostatin receptor selective ligands. NMR and molecular dynamics studies, Int. J. Pept. Protein Res. 46 (1995) 265–278.
[40] B. Leitgeb, Structural investigation of endomorphins by experimental and theoretical methods: hunting for the bioactive conformation, Chem. Biodivers. 4 (2007) 2703–2724.
[41] B.L. Podlogar, M.G. Paterlini, D.M. Ferguson, G.C. Leo, D.A. Demeter, F.K. Brown, A.B. Reitz, Conformational analysis of the endogenous mu-opioid agonist endomorphin-1 using NMR spectroscopy and molecular modeling, FEBS Lett. 439 (1998) 13–20.
[42] S. Fiori, C. Renner, J. Cramer, S. Pegoraro, L. Moroder, Preferred conformation of endomorphin-1 in aqueous and membrane-mimetic environments, J. Mol. Biol. 291 (1999) 163–175.
[43] T.A. Martinek, F. Ötvös, M. Dervarics, G. Tóth, F. Fülöp, Ligand-based prediction of active conformation by 3D-QSAR flexibility descriptors and their application in 3 + 3D-QSAR models, J. Med. Chem. 48 (2005) 3239–3250.
[44] B. Leitgeb, A. Szekeres, Exploring the conformational space of the μ-opioid agonists endomorphin-1 and endomorphin-2, J. Mol. Struct. THEOCHEM (2003), 666–667, 337–344.
[45] F. Ötvös, T. Körtvélyesi, G. Tóth, Structure-activity relationships of endomorphin-1, endomorphin-2 and morphiceptin by molecular dynamics methods, J. Mol. Struct. THEOCHEM (2003), 666–667, 345–353.
[46] D. Tourwé, K. Verschueren, A. Frycia, P. Davis, F. Porreca, V.J. Hruby, G. Tóth, H. Jaspers, P. Verheyden, G. Van Binst, Conformational restriction of Tyr and Phe side chains in opioid peptides: information about preferred and bioactive side-chain topology, Biopolymers 38 (1996) 1–12.
[47] B. Leitgeb, G. Tóth, Aromatic-aromatic and proline-aromatic interactions in endomorphin-1 and endomorphin-2, Eur. J. Med. Chem. 40 (2005) 674–686.
[48] T. Metzger, M.G. Paterlini, P.S. Portoghese, D.M. Ferguson, Application of the message-address concept to the docking of naltrexone and selective naltrexone-derived opioid antagonists into opioid receptor models, Neurochem. Res. 21 (1996) 1287–1294.
[49] D. Strahs, H. Weinstein, Comparative modeling and molecular dynamics studies of the delta, kappa and mu opioid receptors, Protein Eng. 10 (1997) 1019–1038.
[50] I.D. Pogozheva, A.L. Lomize, H.I. Mosberg, Opioid receptor three-dimensional structures from distance geometry calculations with hydrogen bonding constraints, Biophys. J. 75 (1998) 612–634.
[51] K. Palczewski, T. Kumasaka, T. Hori, C.A. Behnke, H. Motoshima, B.A. Fox, B.I. Le Trong, D.C. Teller, T. Okada, R.E. Stenkamp, M. Yamamoto, M. Miyano, Crystal structure of rhodopsin: a G protein-coupled receptor, Science 289 (2000) 739–745.

[52] J. Saunders, Rhodopsin crystal structure: provides information on GPCR-ligand binding in general? Drug Discov. Today 6 (2001) 288–289.
[53] K. Chaturvedi, K.H. Christoffers, K. Singh, R.D. Howells, Structure and regulation of opioid receptors, Biopolymers (Peptide Science) 55 (2001) 334–346.
[54] H.I. Mosberg, C.B. Fowler, Development and validation of opioid ligand-receptor interaction models: the structural basis of mu vs delta selectivity, J. Pept. Res. 60 (2002) 329–335.
[55] K. Fukuda, S. Kato, K. Mori, Location of regions of the opioid receptor involved in selective agonist binding, J. Biol. Chem. 270 (1995) 6702–6709.
[56] K. Fukuda, K. Terasako, S. Kato, K. Mori, Identification of the amino acid residues involved in selective agonist binding in the first extracellular loop of the delta- and mu-opioid receptors, FEBS Lett. 373 (1995) 177–181.
[57] W.W. Wang, M. Shahrestanifar, J. Jin, R.D. Howells, Studies on mu and delta opioid receptor selectivity utilizing chimeric and site-mutagenized receptors, Proc. Natl. Acad. Sci. U.S.A. 92 (1995) 12436–12440.
[58] T. Onogi, M. Minami, Y. Katao, T. Nakagawa, Y. Aoki, T. Toya, S. Katsumata, M. Satoh, DAMGO, a mu-opioid receptor selective agonist, distinguishes between mu- and delta-opioid receptors around their first extracellular loops, FEBS Lett. 357 (1995) 93–97.
[59] A. Mansour, L.P. Taylor, J.L. Fine, R.C. Thompson, M.T. Hoversten, H.I. Mosberg, S.J. Watson, H. Akil, Key residues defining the mu-opioid receptor binding pocket: a site-directed mutagenesis study, J. Neurochem. 68 (1997) 344–353.
[60] R. Spadaccini, P.A. Temussi, Natural peptide analgesics: the role of solution conformation, Cell. Mol. Life Sci. 58 (2001) 1572–1582.
[61] S. Albrizio, A. Carotenuto, C. Fattorusso, L. Moroder, D. Picone, P.A. Temussi, A. D'Ursi, Environmental mimic of receptor interaction: conformational analysis of CCK-15 in solution, J. Med. Chem. 45 (2002) 762–769.
[62] The TINKER software package and documentation is available free at http://dasher.wustl.edu/tinker/.
[63] D. Van der Spoel, E. Lindahl, B. Hess, A.R. van Buuren, E. Apol, P.J. Meulenhoff, D.P. Tieleman, A.L.T.M. Sijbers, K.A. Feenstra, R. van Drunen, H.J.C. Berendsen, Gromacs User Manual version 3.3, 2005 www.gromacs.org.
[64] X. Daura, K. Gademann, B. Jaun, D. Seebach, W.F. van Gunsteren, A.E. Mark, Peptide folding: when simulation meets experiment, Angew. Chem. Int. Ed. Engl. 38 (1999) 236–240.
[65] D.A. Case, T.A. Darden, T.E. Cheatham, C.L. Simmerling, J. Wang, R.E. Duke, R. Luo, K.M. Merz, D.A. Pearlman, M. Crowley, R.C. Walker, W. Zhang, B. Wang, S. Hayik, A. Roitberg, G. Seabra, K.F. Wong, F. Paesani, X. Wu, S. Brozell, V. Tsui, H. Gohlke, L. Yang, C. Tan, L. Mongan, V. Hornak, G. Cui, P. Beroza, D.H. Matthews, C. Schafmeister, W.S. Ross, P.A. Kollman, AMBER 9, University of California, San Francisco, 2006
[66] J. Wang, R.M. Wolf, J.W. Caldwell, P.A. Kollman, Development and testing of a general Amber force field, J. Comp. Chem. 25 (2004) 1157–1174.
[67] W.C. Still, A. Tempczyk, R.C. Hawley, T.S. Hendrickson, Semianalytical treatment of solvation for molecular mechanics and dynamics, J. Am. Chem. Soc. 112 (1990) 6127–6129.
[68] J. Wang, P. Cieplak, P.A. Kollman, How well does a restrained electrostatic potential (RESP) model perform in calculating conformational energies of organic and biological molecules? J. Comp. Chem. 21 (2000) 1049–1074.
[69] W.L. Jorgensen, J. Chandrasekhar, J. Madura, M.L. Klein, Comparison of simple potential functions for simulating liquid water, J. Chem. Phys. 79 (1983) 926–935.
[70] T. Fox, P.A. Kollman, Application of the RESP methodology in the parametrization of organic solvents, J. Phys. Chem. B 102 (1998) 8070–8079.
[71] D. Frishman, P. Argos, Knowledge-based protein secondary structure assignment, Proteins 23 (1995) 566–579.
[72] J.B. Ball, R.A. Hughes, P.F. Alewood, P.R. Andrews, β-Turn topography, Tetrahedron 49 (1993) 3467–3478.
[73] Warren L. DeLano, The PyMOL Molecular Graphics System, DeLano Scientific LLC, San Carlos, CA, USA, (2002) http://www.pymol.org.
[74] A. Borics, R.F. Murphy, S. Lovas, Molecular dynamics simulations of beta-turn forming tetra- and hexapeptides, J. Biomol. Struct. Dyn. 21 (2004) 761–770.
[75] Y. In, K. Minoura, H. Ohishi, H. Minakata, M. Kamigauchi, M. Sugiura, T. Ishida, Comformational comparison of mu-selective endomorphin-2 with its C-terminal free acid in DMSO solution, by 1H NMR spectroscopy and molecular modeling calculation, J. Pept. Res. 58 (2001) 399–412.